INFECTION AND IMMUNITY, Aug. 2006, p. 4401–4408 Vol. 74, No. 8
0019-9567/06/$08.00+0 doi:10.1128/IAI.00637-06

Cytotoxic Necrotizing Factor Type 1 Delivered by Outer Membrane Vesicles of Uropathogenic *Escherichia coli* Attenuates Polymorphonuclear Leukocyte Antimicrobial Activity and Chemotaxis

Jon M. Davis, Humberto M. Carvalho, Susan B. Rasmussen, and Alison D. O'Brien*

Department of Microbiology and Immunology, Uniformed Services University of the Health Sciences, Bethesda, Maryland 20814-4799

Received 20 April 2006/Returned for modification 2 May 2006/Accepted 18 May 2006

Cytotoxic necrotizing factor type 1 (CNF1), a toxin produced by many strains of uropathogenic *Escherichia coli* (UPEC), constitutively activates small GTPases of the Rho family by deamidating a single amino acid within these target proteins. Such activated GTPases not only stimulate actin polymerization within affected cells but also, as we previously reported, decrease membrane fluidity on mouse polymorphonuclear leukocytes (PMNs). In that same investigation we found that this diminished membrane movement impedes the clustering of the complement receptor CD11b/CD18 on PMNs and, in turn, decreases PMN phagocytic capacity and microbicidal activity on PMNs in direct contact with CNF1-expressing UPEC as well as on those in proximity to wild-type UPEC. The latter observation suggested to us that CNF1 is released from neighboring bacteria, although at the time of initiation of the study described here, no specific mechanism for export of CNF1 from UPEC had been described. Here we present evidence that CNF1 is released from the CNF1-expressing UPEC strain CP9 (serotype O4/H5/K54) in a complex with outer membrane vesicles (OMVs) and that these CNF1-bearing vesicles transfer biologically active CNF1 to PMNs and attenuate phagocyte function. Furthermore, we show that CNF1-bearing vesicles act in a dose-dependent fashion on PMNs to inhibit their chemotactic response to formyl-Met-Leu-Phe, while purified CNF1 does not. We conclude that OMVs provide a means for delivery of CNF1 from a UPEC strain to PMNs and thus negatively affect the efficacy of the acute inflammatory response to these organisms.

Uropathogenic *Escherichia coli* (UPEC) strains are responsible for the majority of community-acquired urinary tract infections (UTI) (30). These infections are more frequent among women than among men (10), and treatment costs in the United States exceed one billion dollars annually (30). The mechanisms by which UPEC causes such infections are complex but appear to reflect the impact of multiple bacterial factors linked to UPEC virulence (17). Such microbial components can be grouped by function and include, but are not limited to, adhesins and toxins. Of the adhesins, the best studied are the type 1 fimbriae (6), which mediate binding of the organisms to bladder epithelia (27). The specific functions of toxins, such as α-hemolysin and cytotoxic necrotizing factor type 1 (CNF1), in the pathogenesis of UPEC-mediated UTI are less well understood. However, these two toxins are coexpressed by many UPEC strains (9), and recent animal studies from our laboratory in collaboration with others demonstrated a role for CNF1 in both UTI and acute bacterial prostatitis (28, 29). Moreover, CNF1 is frequently produced by UPEC strains that cause symptomatic UTI in humans (11, 18, 33), although the toxin was first detected in *E. coli* isolates from children with diarrhea (2).

CNF1, a single-chain AB toxin, functions as a deamidase and converts the catalytically active glutamine residue of Rho family GTPases to glutamic acid. The CNF1-catalyzed deamidation of Gln 63 in RhoA and of Gln 61 in Rac and Cdc42 results in the loss of GTPase activity, and these molecules are rendered constitutively active. The Rho GTPases function as molecular switches within cells. When bound to GTP, the Rho family molecules are active and stimulate downstream enzymes such as kinases; after GTP is hydrolyzed to GDP, the Rho GTPases are rendered inactive and their signaling is terminated.

The cycling of Rho family members between the active and inactive forms is essential for the proper functioning of eukaryotic cells such as polymorphonuclear neutrophils (PMNs). In fact, many important antimicrobial features of these phagocytic effector cells of the innate immune system reflect the cycling of Rho family members. For example, Rac1 and Cdc42 are critical for immunoglobulin G-mediated phagocytosis (3), while Rho is important in phagocytosis via CR3 (3). Furthermore, Rac2, an isoform of Rac1, is an essential component of the neutrophil NADPH oxidase used by neutrophils to generate reactive oxygen species and inactivate phagocytosed pathogens (22). Neutrophil chemotaxis is also controlled by Rho GTPases by mechanisms that are now under evaluation through the use of dominant-active and dominant-negative mutants of the Rho GTPases (1, 31, 32). In essence, these studies propose a model of chemotaxis in which a key event is the development of a polarized front on the side of the PMN that faces the chemotactic gradient. This polarization event appears to occur through a positive feedback loop that involves

* Corresponding author. Mailing address: Department of Microbiology and Immunology, Uniformed Services University of the Health Sciences, B4052, 4301 Jones Bridge Road, Bethesda, MD 20814-4799. Phone: (301) 295-3400. Fax: (301) 295-3773. E-mail: aobrien@usuhs.mil.

activation of Rac1, actin polymerization, and an increase in the concentration of phosphatidylinositol 3,4,5-triphosphate (31, 32). Cdc42 is also considered to play a significant role in this scenario of PMN chemotaxis through its interactions with p21-activated kinase. Such a Cdc42–p21-activated kinase association is thought to lead to localized actin polymerization at the neutrophil leading edge and thus to directional sensing and persistent directional migration of these phagocytes (24).

We recently described specific alterations in PMN antimicrobial activity coincident with exposure to CNF1-expressing UPEC strain CP9 (8). In that study we noted that PMNs that were not in direct contact with wild-type CP9 exhibited a phenotype similar to that of PMNs that had direct contact with CP9 when examined microscopically (8). This finding suggested that CNF1 may be released from wild-type UPEC and mediate toxicity in PMNs without direct cell-to-cell contact with UPEC. These observations, combined with the absence of a recognized route for CNF1 release and the role of outer membrane vesicles (OMVs) in the delivery of heat-labile toxin from enterotoxigenic *Escherichia coli* and of the VacA cytotoxin from *Helicobacter pylori* (16, 20, 21), led us to hypothesize that CNF1-expressing UPEC releases outer membrane vesicles that contain the toxin. This theory was recently substantiated by Kouokam et al. (23), who described CNF1 associated with outer membrane vesicles in UPEC. In this investigation, we characterized CNF1-bearing OMVs from a different UPEC strain and assessed the capacity of OMVs to mediate the CNF1-specific effects on PMNs in vivo.

MATERIALS AND METHODS

Bacterial strains and growth conditions. Serogroup O4 uropathogenic *E. coli* strain CP9 and its CNF1-negative isogenic derivative, CP9 *cnf1*, were previously described (29). These strains were transformed with the vector pSX34LacZα, a low-copy-number plasmid with a chloramphenicol resistance marker, to provide experimental consistency between the PMN studies detailed here and those described previously that were done in the presence of chloramphenicol (8). Transformation of CP9 with this vector yielded CP9(pSX34LacZα), and transformation of CP9 *cnf1* generated CP9 *cnf1*(pSX34LacZα); these strains are hereafter referred to as CP9 or wild type and as CP9 *cnf1* or the isogenic mutant, respectively. Bacterial strains were grown overnight in Luria-Bertani (LB) broth at 37°C with shaking. For use in PMN assays, bacteria were then subcultured from overnight broth cultures to LB agar plates that contained 50 μg/ml of chloramphenicol and were harvested after overnight growth as described previously (8).

Western blotting. Membrane vesicle samples were subjected to sodium dodecyl sulfate-polyacrylamide gel electrophoresis (SDS-PAGE) at the acrylamide concentrations indicated and were transferred to nitrocellulose membranes in a semidry apparatus (Bio-Rad). After transfer, membranes were blocked overnight in blocking buffer that consisted of 5% (wt/vol) skim milk in Tris-buffered saline with 0.1% Tween 20. For CNF1 detection, proteins were resolved on 6.5% SDS-polyacrylamide gels and blots were probed with goat anti-CNF1 (1:10,000) as previously described (26). The blots were then incubated with horseradish peroxidase-conjugated porcine anti-goat secondary antibody (Bio-Rad) diluted 1:10,000 in blocking buffer. The O antigen was detected in membrane vesicle preparations (resolved on a 15% SDS-polyacrylamide gel) following transfer to nitrocellulose membranes as described above with rabbit polyclonal anti-O4 (CDC) serum diluted 1:400 in blocking buffer and horseradish peroxidase-conjugated goat anti-rabbit secondary antibody (Bio-Rad) diluted 1:10,000 in blocking buffer. Visualization of both CNF1 and O4 antigen was accomplished by enhanced chemiluminescence (ECL PLUS; Amersham) according to the manufacturer's instructions.

Isolation of outer membrane vesicles. Bacterial outer membrane vesicles were harvested according to the method of Kadurugamuwa and Beveridge (19) with minor modifications. Briefly, bacterial cultures were grown overnight and centrifuged at 8,000 × *g* to pellet bacterial cells, and supernatants were filtered through a 0.2-μm filter to eliminate residual bacteria. The resulting filtrate was centrifuged at 150,000 × *g* in a Beckman Type 70Ti ultracentrifuge rotor for 1.5 h at 4°C; the pellet was washed and resuspended in phosphate-buffered saline (PBS) and stored at −20°C until used. At each stage in the vesicle preparation process, samples were collected, subjected to SDS-PAGE in a 4 to 20% acrylamide gradient gel (Invitrogen), and tested for the presence of CNF1 by Western blotting.

Proteinase K susceptibility assay. To localize vesicle-associated CNF1 in the OMVs, proteinase K susceptibility was tested as previously described (4) with some modifications. Briefly, vesicle samples were incubated at 37°C with 0.5 μg/ml proteinase K, with or without 1% SDS to disrupt vesicle membranes. Samples that contained 1 mM phenylmethylsulfonyl fluoride, a protease inhibitor, and 1% SDS alone served as controls. After 30 min of incubation of these mixtures, SDS-PAGE loading buffer was added to the samples, and then they were immediately heated to 95°C for 5 min. The samples were separated by SDS-PAGE on a 4 to 20% gradient gel and analyzed by Western blotting for the presence of CNF1.

Outer membrane vesicle fractionation. OMVs were isolated as previously described by (16) and resuspended in PBS (pH 7.4). This OMV suspension was used to prepare 1 ml of a 45% OptiPrep (Sigma) solution, which was placed in the bottom of a 12-ml ultracentrifugation tube. Different concentrations of OptiPrep were prepared in 20 mM Tris-HCl solution and layered on top of the 45% solution as follows: 1 ml 35%, 1 ml 30%, 1 ml 25%, 1 ml 20%, 1 ml 15%, 1 ml 10%, and 3 ml 0%. The column gradient was centrifuged at 180,000 × *g* in a Beckman type 40Ti ultracentrifuge rotor for 3 h at 4°C. The fractions were then collected, separated by SDS-PAGE on a 4 to 20% gradient gel, and analyzed by Western blotting to detect *E. coli* O4 and CNF1 antigens.

Enzyme assays. The β-galactosidase activity in the outer membrane vesicle preparation was determined with the Invitrogen Beta-gal assay kit according to the manufacturer's protocol. Alkaline phosphatase activity was detected as described by Maloy et al. (25) with the following modification. The absorbance at 405 nm of each sample was measured in a spectrophotometer, and the concentration of *para*-nitrophenol was calculated based on a molar extinction coefficient of $1.78 \times 10^4\ cm^{-1}\ M^{-1}$. Permeabilized cells were used as a positive control in both enzymatic assays. Protein concentrations in the samples were determined by the bicinchoninic acid method from Pierce according to the manufacturer's instructions.

Determination of KDO content of outer membranes. The 2-keto-3-deoxyoctonate (KDO) content of the outer membrane vesicle preparation was assessed by the thiobarbituric acid method as detailed by Heine (14). The absorbance at 549 nm of each sample was measured spectrophotometrically, and the KDO concentration was calculated based on a molar extinction coefficient of $6.41\ cm^{-1}\ \mu M^{-1}$.

Multinucleation assay. The HEp-2 cell multinucleation assay for CNF1 was done as previously described (26). Purified CNF1 or membrane vesicles derived from either CP9 or CP9 *cnf1* were applied to HEp-2 cells and incubated at 37°C in 5% CO_2 for 4 days. The cells were then fixed, stained with Leukostat (Fisher Scientific), and examined microscopically for the presence of multinucleated HEp-2 cells.

PMN elicitation. Five-week-old female C3H/HeOuJ mice (Jackson Laboratory, Bar Harbor ME) were injected intraperitoneally with 2.5 ml 3% thioglycolate broth (Difco) and then euthanatized 5 hours after injection and subjected to peritoneal lavage to collect the elicited peritoneal white blood cells as previously described (8). The resultant cell exudates were assessed for viability by trypan blue dye exclusion and cell counting with a hemocytometer, and the distribution of cell types was determined microscopically based on Leukostat-stained cell morphology, also as previously described (8). The exudates consisted of 92% granulocytes, 4% mononuclear cells, and 4% lymphocytes. The Uniformed Services University of the Health Sciences Institutional Animal Care and Use Committee approved all animal use protocols.

Bacterial survival in the presence of PMNs. Bacteria were preopsonized in 10% normal mouse serum in Hanks balanced salt solution (HBSS) (BioWhittaker) supplemented with 100 μM Ca^{2+}, 100 μM Mg^{2+}, 0.1% gelatin, 100 μM glucose, and 50 μg/ml chloramphenicol at 37°C prior to the addition of 2×10^6 PMNs. Bacterial strains were added to individual polypropylene tubes at a concentration of 5×10^5 CFU/ml. Tubes with mixtures of bacteria and PMNs were incubated at 37°C and rotated end over end. In some cases, bacterial culture supernatants were added to these mixtures. These supernatants were prepared as follows. One milliliter of an overnight growth of the specific bacterial culture was centrifuged at 8,000 × *g* for 5 min at 4°C in a bench-top centrifuge (Eppendorf). The supernatant was removed and filtered through a 0.2-μm low-protein binding syringe filter. Filtrate sterility was assessed by culturing an aliquot overnight in LB broth supplemented with 50 μg/ml chloramphenicol. A 2-μl aliquot of this of the sterile filtrate was added to the bacterium-PMN mixture described above.

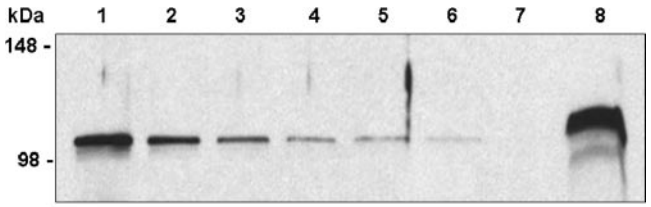

Lane	Description	ng of CNF1 / well (Image J)
1	Purified CNF1 (76 ng)	76.9
2	Purified CNF1 (38 ng)	35.6
3	Purified CNF1 (19 ng)	20.1
4	Purified CNF1 (9.5 ng)	9.9
5	Overnight supernatant	9.1
6	Filtrate	0.2
7	Ultracentrifugation supernatant	undetectable
8	Ultracentrifugation sediment	146.4

FIG. 1. Immunoblot analysis of culture supernatant. The amount of CNF1 detected in culture fractions by Western blotting was extrapolated from a standard curve of the pixel densities of bands observed on the same immunoblot with known quantities of CNF1 (lanes 1 through 4). Culture supernatant (lane 5) was centrifuged and then filtered through a 0.2-μm filter (lane 6). Ultracentrifugation of the resultant filtrate yielded the ultracentrifugation supernatant (lane 7) and the ultracentrifugation sediment (lane 8).

This filtrate volume was selected after calculating the volume of overnight culture that would yield a bacterial concentration equivalent to the concentration of wild-type bacteria present at the end of the bacterial survival experiment. When outer membrane vesicle preparations were added to the mixtures, 2 μl of the vesicle preparation was used in place of a sterile culture filtrate.

PMN chemotaxis. The chemotactic response of PMNs to formyl-Met-Leu-Phe (fMLP) (Sigma) was measured with the QCM Chemotaxis 3-μm 96-well cell migration assay (ECM515) from Chemicon International according to the manufacturer's protocol. Briefly, PMNs were preincubated for 20 min with either membrane vesicles from CP9 or CP9 *cnf1*, purified CNF1, or HBSS. The amount of CNF1 in the OMVs derived from CP9 was quantified by Western blotting based on a standard curve of purified CNF1 run in parallel. Duplicate samples of each mixture were applied to the upper migration chamber; a chemical gradient between the upper and lower chambers was established by placing 1×10^{-4} M fMLP in the lower chamber. The cells were incubated for 1 h at 37°C in an incubator that contained 5% CO_2, and the cells were then fluorescently labeled according to the manufacturer's instructions. The fluorescence intensity of each sample was measured on a SpectraMax M2 fluorescent microplate reader with SoftMax Pro software (Molecular Devices). The number of migrated PMNs was calculated based on a standard curve run in parallel. The response of PMNs treated with membrane vesicles or purified CNF1 was normalized to that of untreated PMNs (with HBSS) prior to data analysis.

Electron microscopy. OMVs were prepared for electron microscopy according to previously published methods (12, 13). In essence, outer membrane vesicles were fixed in a mixture of 2% paraformaldehyde and 2% glutaraldehyde in 0.1 M cacodylate buffer with 2% sucrose. The samples were then washed in 0.1 M cacodylate buffer and postfixed in 1% OsO_4 in 0.1 M cacodylate buffer with 1% $K_3Fe(CN)_6$ and 1% sucrose (pH 7.4) to improve membrane contrast. After fixation, the samples were washed again and processed in Araldite plastic embedding medium (12, 13). Ultrathin sections (70 to 80 nm) were obtained from the Araldite blocks with a Diatome diamond knife and collected on copper hexagonal grids. Sections were stained with uranyl acetate (30 min) and lead citrate (5 min) and examined in a CM 100 Philips/FEI electron microscope at a beam voltage of 80 hK, and photomicrographs of the sections were taken.

Immunofluorescence. PMNs (1×10^6) and outer membrane vesicles (2 μg total protein) were coincubated for 150 min with end-over-end tumbling. All steps of the incubation were conducted at 4°C to prevent internalization by PMNs of any bound membrane vesicles. During the final 45 min of the coincubation of these PMN-OMV mixtures, samples were transferred to poly-D-lysine (3 mg/ml; Sigma)-coated coverslips that had been placed on the bottoms of 24-well tissue culture plates. The coverslips that contained the samples were then washed to remove unbound membrane vesicles, fixed in 3% freshly prepared paraformaldehyde (EMS) for 30 min at 37°C, and blocked overnight at 4°C in blocking buffer that consisted of 3% bovine serum albumin and 10% heat-inactivated normal goat serum (Sigma). Rabbit polyclonal anti-O4 serum was diluted 1:200 in blocking buffer and applied to the cells for 1 h at room temperature. The cells were then washed in PBS, and goat anti-rabbit Alexa 488 (Molecular Probes) was applied at 5 μg/ml in blocking buffer for 1 h at room temperature. The cells were washed again in PBS and the coverslips mounted with Fluormount G (Southern Biotech) onto glass slides. The stained cells were viewed on an Olympus microscope (model BX60) equipped for epifluorescence with a filter for fluorescein isothiocyanate (Chroma Technologies, set 41001) detection. Images were obtained with a SPOT RT charge-coupled-device digital camera made by Diagnostic Instruments, Inc. The final images were prepared with ImageJ 1.34g (W. S. Rasband, National Institutes of Health, Bethesda, Maryland; http://rsb.info.nih.gov/ij/, 1997 to 2005).

Statistical analysis. Data were evaluated for statistical significance by analysis of variance (ANOVA) after plotting the residuals to determine that the data were normally distributed. All calculations were done with the SPSS 11.0 program in consultation with our in-house statistician, Cara Olsen.

RESULTS

Outer membrane vesicles from CP9 are complexed with CNF1. Kouokam and colleagues recently demonstrated, coincident with this investigation, that CNF1 is present in outer membrane vesicles derived from UPEC strain J96 (23). Our work to describe the export of CNF1 from UPEC was conducted with strain CP9. We used a previously described method to isolate OMVs from CP9 and CP9 *cnf1* culture supernatants and then applied Western blot analysis to detect CNF1 in various cellular fractions (Fig. 1). CNF1 was detectable in the sedimented cellular fraction (Fig. 1, lane 8), while CNF1 was not detectable in the supernatant following ultracentrifugation (Fig. 1, lane 7). That CNF1 was sedimented out of suspension by ultracentrifugation, suggesting that it existed as a complex with the outer membrane fraction rather than as a soluble protein. Further characterization of the pellet demonstrated the presence of the KDO sugar of lipopolysaccharide and the O4 antigen, which are both components of the outer membrane in CP9 (Table 1 and Fig. 2). We reasoned that if membrane vesicles derived from the outer membrane were present in the sedimented fraction, they would likely contain a fraction of the periplasmic contents such as alkaline phosphatase. Therefore, we measured the alkaline phosphatase

TABLE 1. Biochemical characterization of OMVs derived from UPEC strain CP9 and its isogenic CNF1-negative mutant[a]

Bacterial source	Prepn	KDO (μg/ml)	β-Galactosidase (nmol/min/μg, 10^{-3})	Alkaline phosphatase (nmol/min/μg, 10^{-3})
CP9	Supernatant[b]		<5.00[c]	ND[d]
	OMV	30.03	<5.00	1.99 ± 0.17
	Permeabilized cells		70.19 ± 0.89	5.71 ± 0.60
CP9 *cnf1*	Supernatant		<5.00	ND
	OMV	25.53	<5.00	2.04 ± 0.21

[a] Data are shown as the means ± standard deviations from three independent determinations calculated from the molar extinction coefficient as described in Materials and Methods.
[b] Clarified, filtered culture supernatant prior to ultracentrifugation (12× concentrated).
[c] Below the limit of detection.
[d] ND, not determined.

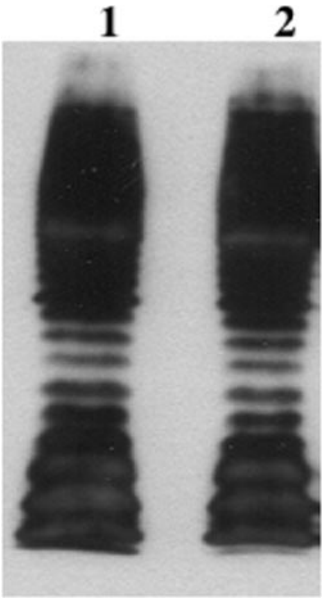

FIG. 2. Ultracentrifuged culture sediment was analyzed by immunoblotting for the presence of the O4 antigen as a marker of the bacterial outer membrane. Lane 1, CP9 pellet; lane 2, CP9 *cnf1* pellet.

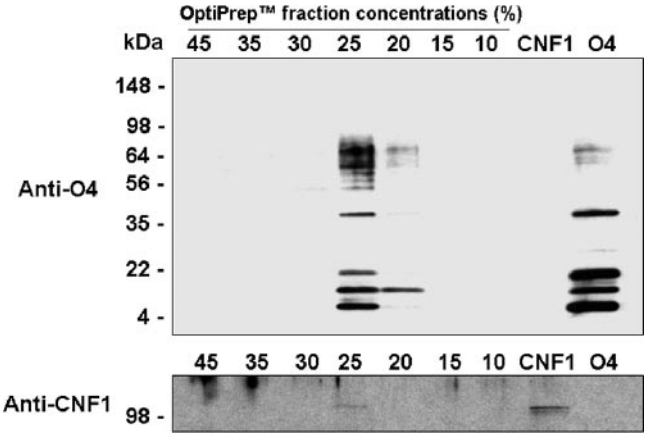

FIG. 3. Density gradient separation of culture supernatant. Culture supernatants were clarified by centrifugation and filtration through a 0.2-μm filter and placed on the bottom of a density gradient constructed with OptiPrep. The various OptiPrep fractions were analyzed by immunoblotting after ultracentrifugation for the presence of CNF1 and O4 antigen. Purified CNF1 toxin (100 ng) (lane CNF1) and an overnight culture of CP9 (20 ml) (lane O4) were used as positive controls for the CNF1 and O4 antibodies, respectively.

activity of the sedimented fraction and found that it did indeed possess alkaline phosphatase activity (Table 1). In addition, neither the ultracentrifuged sediment (putative OMVs) nor the starting supernatant contained measurable quantities of β-galactosidase, findings consistent with scant cytoplasmic contamination in these fractions (Table 1). In an effort to more rigorously demonstrate that CNF1 was associated with the vesicle fraction, we constructed a density gradient and used it to separate vesicles from potential CNF1 multimers that might have been present in the starting material. Material obtained from the 25% fraction contained both CNF1 and the O4 antigen, a finding that indicates that CNF1 is part of a fraction with a buoyant density similar to that of the outer membrane (Fig. 3). We next sought to determine the location of CNF1 relative to the OMV through the application of a protease protection assay in which CNF1 located within the OMV would be protected from proteinase K degradation. We found that CNF1 was present on the exterior of the OMV (Fig. 4). In aggregate, these biochemical data show that the sediment formed after ultracentrifugation of the culture supernatant of UPEC strain CP9 is composed of outer membrane vesicles that contain periplasmic contents and CNF1.

Vesicles are observed by electron microscopy. Transmission electron microscopy was used to assess whether OMVs were indeed present in the CP9 culture supernatant pellet after ultracentrifugation. The transmission electron microscopy images of this sedimented material revealed the presence of many vesicles but, as predicted, no intact bacteria (Fig. 5A). Most of the vesicles were less than 200 nm in size and were typically spherical in shape (Fig. 5A). However, some OMVs appeared to have fused with each other to generate larger, irregularly shaped vesicles (Fig. 5B).

Multinucleation of HEp-2 cells by OMVs. HEp-2 cells display a characteristic phenotype of multinucleation and enlargement when intoxicated with CNF1. We used this standard assay of CNF1 activity to determine whether the membrane vesicles derived from CP9 contained biologically active CNF1. We incubated HEp-2 cells with either purified CNF1 or membrane vesicles from the wild-type strain or the isogenic mutant. We observed that HEp-2 cells displayed the characteristic features of CNF1 intoxication, such as cellular enlargement and multinucleation, when incubated with purified CNF1 (Fig. 5C) or membrane vesicles from CP9 (Fig. 5D). Cells incubated with membrane vesicles derived from the isogenic mutant exhibited cellular morphology similar to that of HEp-2 cells that were incubated with medium only (Fig. 5, compare panels E and F). These results demonstrate that membrane vesicles derived from wild-type UPEC strain CP9 contain biologically active CNF1.

OMVs interact with mouse PMNs. The presence of outer membrane vesicles in the culture supernatants and the detrimental effect of the wild-type supernatant on PMN microbici-

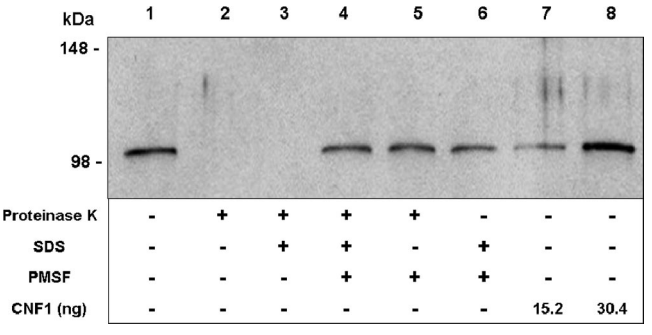

FIG. 4. Protease protection assay. Purified OMVs were treated with proteinase K in the presence and absence of either 1% SDS or phenylmethylsulfonyl fluoride (PMSF). The presence of CNF1 in each of the conditions was determined by immunoblot analysis with polyclonal anti-CNF1 antibody.

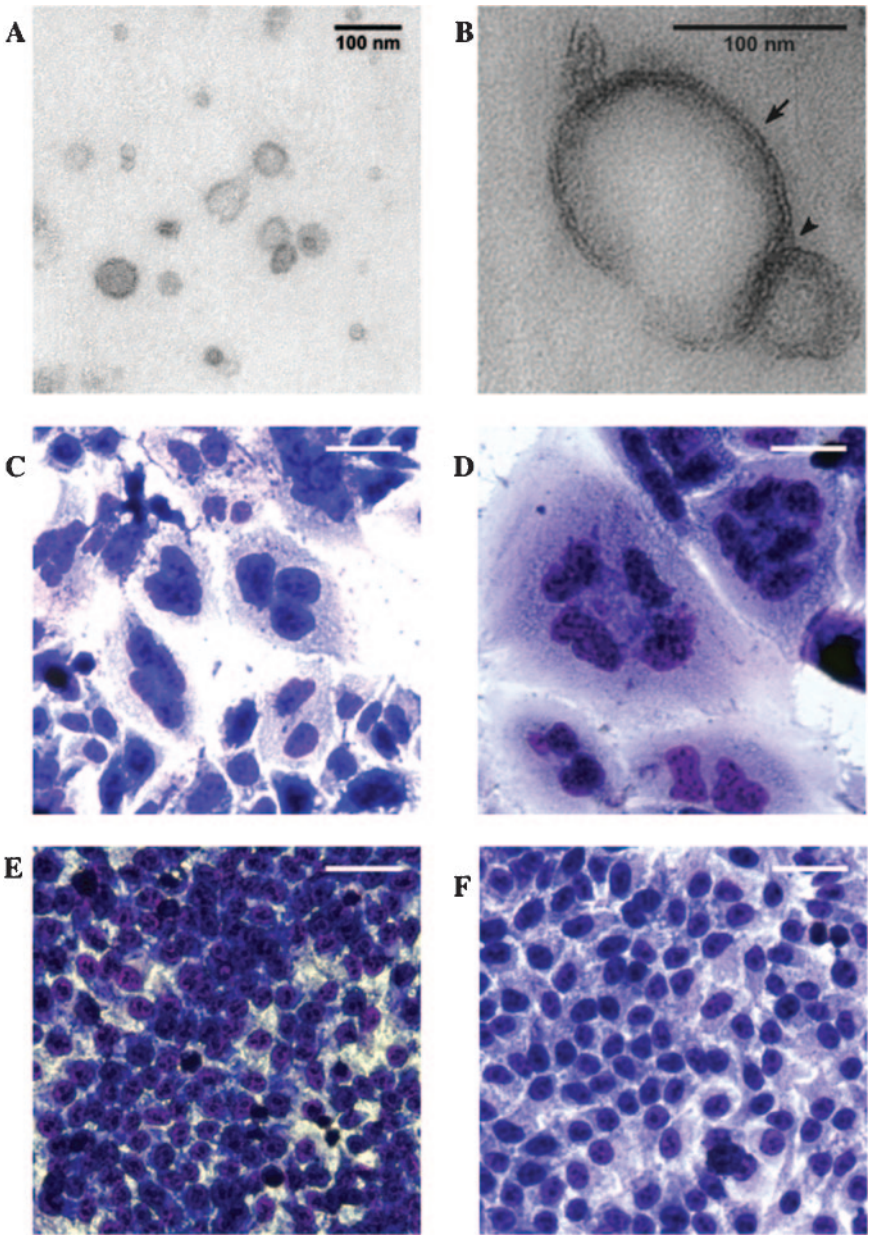

FIG. 5. Electron micrograph of and activity associated with membrane vesicles prepared from CP9. Culture supernatants were prepared by centrifugation and filtration to remove bacterial cells, and insoluble material was then sedimented by ultracentrifugation. The resulting pellet was embedded and prepared for electron microscopy. (A) Wide-field view of membrane vesicle preparation from CP9, showing many vesicles of various diameters. (B) Vesicles from CP9 that illustrate the fusion of a large and small vesicle (arrowhead) and the bilayer structure of the vesicles (arrow). (C to F) HEp-2 cells exposed to purified CNF1 (C), OMVs from CP9 (D), OMVs derived from CP9 *cnf1* (E), or medium alone (F). Bars in panels C to F, 50 μm.

dal activity led us to investigate whether CP9 OMVs could interact with PMNs. To address that question, PMNs and OMVs were coincubated and then immunostained with anti-O4 antibody to detect membrane components on the PMN surface. As depicted in Fig. 6, the outer membrane vesicles derived from CP9 were associated with the mouse PMNs. We then theorized that the association of vesicles with PMNs could serve as a means to direct CNF1 to PMNs and that such OMV targeting was responsible for the altered microbicidal activity seen in PMNs treated with clarified supernatant. To test this idea, PMNs were cocultured with bacteria and membrane vesicles derived from either CP9 or CP9 *cnf1*. The concentration of viable bacteria at various time points was then determined. When CP9 *cnf1* was coincubated with PMNs in the presence of wild-type OMVs, the net replication of the mutant increased to levels comparable to that of CP9 coincubated with PMNs (Fig. 7). However, when OMVs from the isogenic mutant were added back to the PMNs cultured with CP9 *cnf1*, diminished survival over time of the mutant compared to the wild type coincubated with PMNs was observed ($P < 0.01$) (Fig. 7). Collectively,

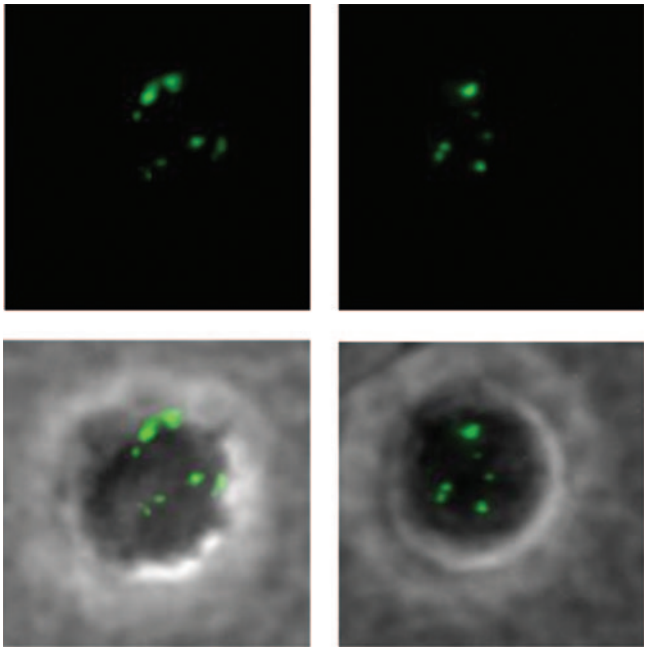

FIG. 6. Fluorescently labeled outer membrane vesicles interact with PMNs. Outer membrane vesicles prepared from CP9 were coincubated with PMNs at 4°C. Fluorescent images of two different cells (lower panels) were obtained following immunostaining for the O4 antigen contained in outer membrane vesicles (green); corresponding phase-contrast images (upper panels) of the PMN are also shown. The coincubation of PMNs with the outer membrane vesicle preparation resulted in the presence of punctate staining of the O4 antigen along the surface of the PMN, indicating the presence of the O4 antigen on the PMN membrane. The corresponding control PMNs not incubated with outer membrane vesicles did not stain.

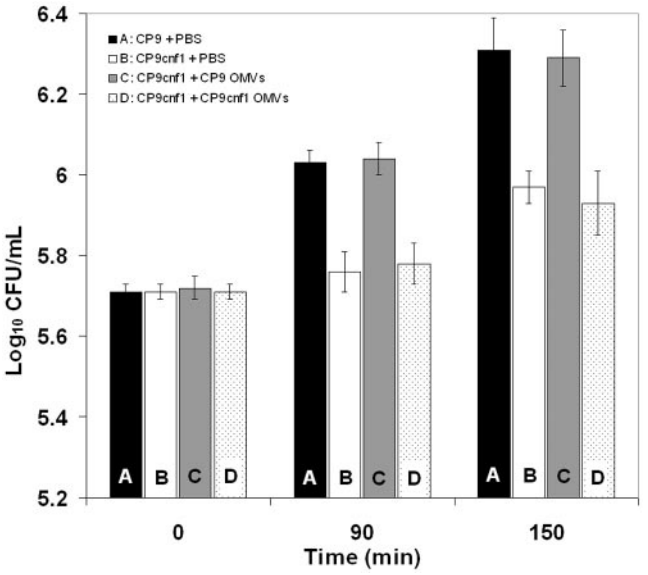

FIG. 7. OMVs from CNF1-expressing CP9 reduce PMN antimicrobial capacity. The net replication of the wild-type strain (A) and the *cnf1* mutant of CP9 (B) coincubated with PBS was compared to the net replication of CNF1-negative CP9 coincubated with purified OMVs from wild-type CP9 (C) or OMVs from *cnf1* isogenic mutant UPEC (D) in the presence of PMNs. The results are from three experiments performed in triplicate and are shown as the mean $\log_{10}$ CFU/ml viable bacteria; the error bars indicate the 95% confidence intervals for each condition. The data were analyzed by ANOVA, and the differences (wild type versus mutant in all conditions) are significant ($P < 0.01$).

these results suggest that wild-type CP9 releases CNF1 complexed with OMVs and that these CNF1-bearing vesicles interact with and diminish the antimicrobial activity of PMNs.

CNF1-bearing OMVs alter PMN chemotaxis. The effect of OMVs from wild-type CP9 on the PMN antimicrobial response led us to examine whether other features of PMN physiology were altered by wild-type OMVs. For that purpose, we elected to examine PMN chemotaxis, because this phagocyte function is controlled in part by the Rho family GTPases and because CNF1 constitutively activates this family of GTP binding proteins. When the chemotaxis of PMNs coincubated with OMVs from CP9 was measured relative to that of the untreated controls after 1 h, the PMNs coincubated with wild-type OMVs demonstrated a dose-dependent and statistically significant ($P < 0.05$) diminution in chemotaxis compared to PMNs coincubated with OMVs from the isogenic mutant (Fig. 8). Although OMVs from the isogenic mutant reduced PMN chemotaxis at the highest concentration tested, this effect was not statistically significant and was likely due to bacterial products in the OMVs competing with the fMLP gradient. Additionally, we observed that an amount of purified CNF1 equivalent to that delivered by OMVs did not affect chemotaxis (Fig. 8). In total, these findings demonstrate that OMVs that contain CNF1 dampen the chemotactic response of PMNs and indicate that OMVs may intoxicate PMNs more efficiently than purified toxin.

DISCUSSION

In this study, we have presented evidence that CNF1 from UPEC strain CP9 is associated with an acellular fraction that contains membrane vesicles with characteristics of the bacterial outer membrane. In addition, we showed that mouse PMNs exhibit an altered phenotype when coincubated with membrane vesicles. Specifically, we demonstrated that PMNs treated with wild-type membrane vesicles displayed a reduced antimicrobial capacity and a diminished chemotactic response compared to PMNs treated with membrane vesicles from the *cnf1* isogenic mutant. These findings indicate that biologically active CNF1 from UPEC is delivered to PMNs via outer membrane vesicles and support and extend the report of Kouokam et al. (23).

Two alternative explanations for our finding of CNF1 in the vesicle fraction are also possible. First, bacterial lysis may have released cytoplasmic contents that included CNF1, or second, CNF1 may have formed multimers or a precipitate that sedimented during ultracentrifugation. The argument against the first possibility is the finding of negligible levels of β-galactosidase activity in the vesicle fraction under our experimental conditions. Our line of reasoning against the second scenario, the possible formation of CNF1 multimers, is the observation that CNF1 and OMVs were detected in the same density gradient fraction. We believe that had CNF1 formed multimers large enough to be sedimented during ultracentrifugation, then CNF1 would have been detected in density gradient fractions that did not contain OMVs. The fact that CNF1 and OMVs were detected only in the same fraction strongly sup-

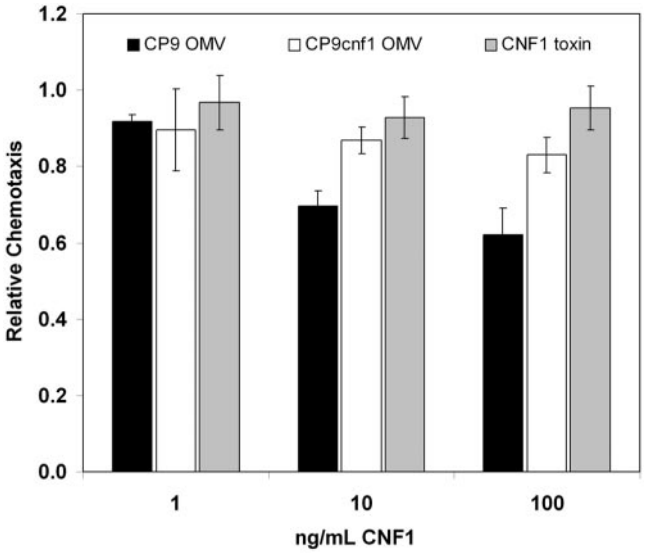

FIG. 8. PMN chemotaxis is inhibited in the presence of CNF1-containing OMVs. The PMN chemotactic response to fMLP was evaluated in Boyden-type chambers following preincubation of PMNs with OMVs derived from wild-type CP9 (black bars), *cnf1* isogenic mutant UPEC (white bars), or purified CNF1 (gray bars). PMNs were allowed to respond to the fMLP gradient for 1 h; the number of migrated PMNs from each condition was determined fluorescently based on a standard curve. The data were then normalized relative to those for the untreated control (with HBSS). The results of three experiments performed in duplicate are shown as the mean normalized chemotactic index; error bars indicate the standard errors of the means. The normalized data were analyzed by ANOVA, and the differences (CP9 OMV versus purified toxin and CP9 OMV at 1 ng/ml versus CP9 OMV at 10 ng/ml) are significant ($P < 0.05$).

ports the conclusion that CNF1 is intimately associated with OMVs.

We propose that for OMVs to convey biologically active toxin to the PMN, these vesicles must first interact with these phagocytes. The membrane vesicles appeared to fulfill this requirement as evaluated by coincubation studies with mouse PMNs. Indeed, in these coincubation experiments, we noted by immunostaining the formation of many punctate patches of O4 antigen on the PMNs. This observation suggests that the membrane vesicles may have merged with the PMNs. Kesty and colleagues also reported similar interactions between the toxin-bearing vesicles of enterotoxigenic *E. coli* and eukaryotic cells (21). That our vesicles contained biologically active toxin was demonstrated by three separate phenotypic assays. First, when HEp-2 cells were incubated with OMVs derived from CP9, these cells demonstrated a pattern of multinucleation similar to that of HEp-2 cells incubated with purified toxin. The multinucleation pattern is a classic phenotype of CNF1 intoxication in HEp-2 cells. Second, the net replication of CP9 *cnf1* was significantly less than the net replication of CP9 in the presence of PMNs and OMVs collected from the *cnf1* isogenic mutant. However, when wild-type vesicles were substituted for mutant vesicles in similar studies, the net replication of the *cnf1* isogenic mutant was essentially equivalent to that of the wild-type CP9. Finally, the chemotactic response of PMNs to fMLP was altered in a dose-dependent fashion following treatment with CNF1-bearing vesicles but not when PMNs were treated with membrane vesicles from the CNF1 mutant or purified toxin. The results of our chemotaxis experiments revealed that CNF1-bearing vesicles diminish PMN chemotaxis in response to chemical attractants and indicated that CNF1 acts directly on PMNs.

The constitutive activation of Rho family GTPases by CNF1 provides a potential explanation for our observation of diminished chemotaxis of PMNs in the presence of CNF1-containing OMVs. Chemotaxis is a complex process in which neutrophils must detect the chemotactic stimuli and become oriented in a polarized fashion (32). The precise mechanism that controls this cellular response is unclear, but Rho family GTPases do have distinct roles in this process (1, 24, 31, 32). For example, Srinivasan and colleagues reported that differentiated HL-60 cells transfected with a dominant active form of Rac (RacV12) demonstrated a uniform distribution of activated Rac compared to untransfected control cells, which showed a more polarized distribution of Rac, in response to a gradient of fMLP (31). In addition, Allen and colleagues detected a decreased chemotactic response in macrophages microinjected with dominant active RhoA, Rac1, and Cdc42 (1). Those investigators hypothesized that constitutively active RhoA would be antagonistic to Rac and the development of a polarized morphology. Indeed, this theory was proven by Xu et al., who used differentiated HL-60 cells transfected with dominant active RhoA to show that these transfected cells failed to develop a polarized morphology or undergo chemotaxis in response to fMLP (32). Based on these earlier observations and our own studies, we speculate that the diminished chemotaxis demonstrated by neutrophils exposed to wild-type vesicles reflects the constitutive activation of Rho GTPases by CNF1. Specifically, we propose that the CNF1-catalyzed deamidation of Rho GTPases results in a reduction in the capacity of intoxicated neutrophils to establish and maintain a polarized front in response to a gradient of fMLP.

When we exposed PMNs to purified CNF1, we did not detect any effect on chemotaxis. Similar results were obtained by Hofman and colleagues, who saw negligible effects from CNF1 on migration of human neutrophils through polarized T24 cell monolayers (15). In contrast, as discussed above, we observed a clear chemotactic effect on PMNs in response to CNF1-containing outer membrane vesicles. The delivery of CNF1 via membrane vesicles may target the toxin to the PMN membrane and possibly the cytosol more effectively than the receptor-mediated pathway previously described for CNF1 (5, 7). The detection of CNF1 associated with outer membrane vesicles derived from UPEC strain CP9 and the observed biological effects of such vesicles on PMNs suggest that OMVs may provide an important vehicle for delivery of CNF1 by UPEC during infection. Such delivery of CNF1 may, in turn, lead to interference with PMN antimicrobial capacity and chemotaxis.

ACKNOWLEDGMENTS

This work was supported by grant AI38281 from the National Institutes of Health.

We thank Louise D. Teel for critical review of the manuscript and Gertrud Goping for her assistance with electron microscopy.

The opinions or assertions contained herein are those of the authors and are not to be construed as the views of the Department of Defense.

REFERENCES

1. **Allen, W. E., D. Zicha, A. J. Ridley, and G. E. Jones.** 1998. A role for Cdc42 in macrophage chemotaxis. J. Cell Biol. **141:**1147–1157.
2. **Caprioli, A., V. Falbo, L. G. Roda, F. M. Ruggeri, and C. Zona.** 1983. Partial purification and characterization of an *Escherichia coli* toxic factor that induces morphological cell alterations. Infect. Immun. **39:**1300–1306.
3. **Caron, E., and A. Hall.** 1998. Identification of two distinct mechanisms of phagocytosis controlled by different Rho GTPases. Science **282:**1717–1721.
4. **Cheng, L. W., and O. Schneewind.** 2000. *Yersinia enterocolitica* TyeA, an intracellular regulator of the type III machinery, is required for specific targeting of YopE, YopH, YopM, and YopN into the cytosol of eukaryotic cells. J. Bacteriol. **182:**3183–3190.
5. **Chung, J. W., S. J. Hong, K. J. Kim, D. Goti, M. F. Stins, S. Shin, V. L. Dawson, T. M. Dawson, and K. S. Kim.** 2003. 37-kDa laminin receptor precursor modulates cytotoxic necrotizing factor 1-mediated RhoA activation and bacterial uptake. J. Biol. Chem. **278:**16857–16862.
6. **Connell, I., W. Agace, P. Klemm, M. Schembri, S. Marild, and C. Svanborg.** 1996. Type 1 fimbrial expression enhances *Escherichia coli* virulence for the urinary tract. Proc. Natl. Acad. Sci. USA **93:**9827–9832.
7. **Contamin, S., A. Galmiche, A. Doye, G. Flatau, A. Benmerah, and P. Boquet.** 2000. The p21 Rho-activating toxin cytotoxic necrotizing factor 1 is endocytosed by a clathrin-independent mechanism and enters the cytosol by an acidic-dependent membrane translocation step. Mol. Biol. Cell **11:**1775–1787.
8. **Davis, J. M., S. B. Rasmussen, and A. D. O'Brien.** 2005. Cytotoxic necrotizing factor type 1 production by uropathogenic *Escherichia coli* modulates polymorphonuclear leukocyte function. Infect. Immun. **73:**5301–5310.
9. **Falbo, V., M. Famiglietti, and A. Caprioli.** 1992. Gene block encoding production of cytotoxic necrotizing factor 1 and hemolysin in *Escherichia coli* isolates from extraintestinal infections. Infect. Immun. **60:**2182–2187.
10. **Foxman, B.** 2002. Epidemiology of urinary tract infections: incidence, morbidity, and economic costs. Am. J. Med. **113**(Suppl. 1A)**:**5S–13S.
11. **Foxman, B., L. Zhang, K. Palin, P. Tallman, and C. F. Marrs.** 1995. Bacterial virulence characteristics of *Escherichia coli* isolates from first-time urinary tract infection. J. Infect. Dis. **171:**1514–1521.
12. **Goping, G., H. B. Pollard, O. M. Adeyemo, and G. A. Kuijpers.** 1995. Effect of MPTP on dopaminergic neurons in the goldfish brain: a light and electron microscope study. Brain Res. **687:**35–52.
13. **Goping, G., S. Yedgar, H. B. Pollard, and G. A. Kuijpers.** 1992. Flat embedding and immunolabelling of SW 1116 colon carcinoma cells in LR white: an improved technique in light and electron microscopy. Microsc. Res. Tech. **21:**1–9.
14. **Heine, H. S.** 1993. Biosynthesis of enterobacterial common antigen. The ECA-trace phenotype of *Salmonella typhimurium* and the role of the *rfe* gene in O8 side-chain synthesis in *Escherichia coli*. Ph.D. thesis. Uniformed Services University of the Health Sciences, Bethesda, Md.
15. **Hofman, P., G. Flatau, E. Selva, M. Gauthier, G. Le Negrate, C. Fiorentini, B. Rossi, and P. Boquet.** 1998. *Escherichia coli* cytotoxic necrotizing factor 1 effaces microvilli and decreases transmigration of polymorphonuclear leukocytes in intestinal T84 epithelial cell monolayers. Infect. Immun. **66:**2494–2500.
16. **Horstman, A. L., and M. J. Kuehn.** 2000. Enterotoxigenic *Escherichia coli* secretes active heat-labile enterotoxin via outer membrane vesicles. J. Biol. Chem. **275:**12489–12496.
17. **Johnson, J. R.** 1991. Virulence factors in *Escherichia coli* urinary tract infection. Clin. Microbiol. Rev. **4:**80–128.
18. **Johnson, J. R., F. Scheutz, P. Ulleryd, M. A. Kuskowski, T. T. O'Bryan, and T. Sandberg.** 2005. Phylogenetic and pathotypic comparison of concurrent urine and rectal *Escherichia coli* isolates from men with febrile urinary tract infection. J. Clin. Microbiol. **43:**3895–3900.
19. **Kadurugamuwa, J. L., and T. J. Beveridge.** 1995. Virulence factors are released from *Pseudomonas aeruginosa* in association with membrane vesicles during normal growth and exposure to gentamicin: a novel mechanism of enzyme secretion. J. Bacteriol. **177:**3998–4008.
20. **Keenan, J., T. Day, S. Neal, B. Cook, G. Perez-Perez, R. Allardyce, and P. Bagshaw.** 2000. A role for the bacterial outer membrane in the pathogenesis of *Helicobacter pylori* infection. FEMS Microbiol. Lett. **182:**259–264.
21. **Kesty, N. C., K. M. Mason, M. Reedy, S. E. Miller, and M. J. Kuehn.** 2004. Enterotoxigenic *Escherichia coli* vesicles target toxin delivery into mammalian cells. EMBO J. **23:**4538–4549.
22. **Kim, C., and M. C. Dinauer.** 2001. Rac2 is an essential regulator of neutrophil nicotinamide adenine dinucleotide phosphate oxidase activation in response to specific signaling pathways. J. Immunol. **166:**1223–1232.
23. **Kouokam, J. C., S. N. Wai, M. Fällman, U. Dobrindt, J. Hacker, and B. E. Uhlin.** 2006. Active cytotoxic necrotizing factor 1 associated with outer membrane vesicles from uropathogenic *Escherichia coli*. Infect. Immun. **74:**2022–2030.
24. **Li, Z., M. Hannigan, Z. Mo, B. Liu, W. Lu, Y. Wu, A. V. Smrcka, G. Wu, L. Li, M. Liu, C. K. Huang, and D. Wu.** 2003. Directional sensing requires G $\beta\gamma$-mediated PAK1 and PIX α-dependent activation of Cdc42. Cell **114:**215–227.
25. **Maloy, S. R., V. J. Stewart, and R. K. Taylor.** 1996. Genetic analysis of pathogenic bacteria: a laboratory manual. Cold Spring Harbor Laboratory Press, Plainview, N.Y.
26. **Mills, M., K. C. Meysick, and A. D. O'Brien.** 2000. Cytotoxic necrotizing factor type 1 of uropathogenic *Escherichia coli* kills cultured human uroepithelial 5637 cells by an apoptotic mechanism. Infect. Immun. **68:**5869–5880.
27. **Mulvey, M. A., J. D. Schilling, J. J. Martinez, and S. J. Hultgren.** 2000. Bad bugs and beleaguered bladders: interplay between uropathogenic *Escherichia coli* and innate host defenses. Proc. Natl. Acad. Sci. USA **97:**8829–8835.
28. **Rippere-Lampe, K. E., M. Lang, H. Ceri, M. Olson, H. A. Lockman, and A. D. O'Brien.** 2001. Cytotoxic necrotizing factor type 1-positive *Escherichia coli* causes increased inflammation and tissue damage to the prostate in a rat prostatitis model. Infect. Immun. **69:**6515–6519.
29. **Rippere-Lampe, K. E., A. D. O'Brien, R. Conran, and H. A. Lockman.** 2001. Mutation of the gene encoding cytotoxic necrotizing factor type 1 (*cnf1*) attenuates the virulence of uropathogenic *Escherichia coli*. Infect. Immun. **69:**3954–3964.
30. **Russo, T. A., and J. R. Johnson.** 2003. Medical and economic impact of extraintestinal infections due to *Escherichia coli*: focus on an increasingly important endemic problem. Microbes. Infect. **5:**449–456.
31. **Srinivasan, S., F. Wang, S. Glavas, A. Ott, F. Hofmann, K. Aktories, D. Kalman, and H. R. Bourne.** 2003. Rac and Cdc42 play distinct roles in regulating $PI(3,4,5)P_3$ and polarity during neutrophil chemotaxis. J. Cell Biol. **160:**375–385.
32. **Xu, J., F. Wang, K. A. Van, P. Herzmark, A. Straight, K. Kelly, Y. Takuwa, N. Sugimoto, T. Mitchison, and H. R. Bourne.** 2003. Divergent signals and cytoskeletal assemblies regulate self-organizing polarity in neutrophils. Cell **114:**201–214.
33. **Yamamoto, S., T. Tsukamoto, A. Terai, H. Kurazono, Y. Takeda, and O. Yoshida.** 1995. Distribution of virulence factors in *Escherichia coli* isolated from urine of cystitis patients. Microbiol. Immunol. **39:**401–404.

Editor: J. T. Barbieri